

Optimal Cost Minimization Strategy for Fuel Cell Hybrid Electric Vehicles Based on Decision Making

Ravikiran Narsingrao Patange¹ and Prof. K. M. Mahajan²

M.Tech Scholar, Department of EE¹

HoD, Department of EE²

KCES's College of Engineering and Management, Jalgaon, Maharashtra, India

Abstract: *The low economy of fuel cell hybrid electric vehicles is a big challenge to their wide usage. A road, health, and price-conscious optimal cost minimization strategy based on decision making framework was developed to decrease their overall cost. First, an online applicable cost minimization strategy was developed to minimize the overall operating costs of vehicles including the hydrogen cost and degradation costs of fuel cell and battery. Second, a decision making framework composed of the driving pattern recognition-enabled, prognostics-enabled, and price prediction-enabled decision makings, for the first time, was built to recognize the driving pattern, estimate health states of power sources and project future prices of hydrogen and power sources. Based on these estimations, optimal equivalent cost factors were updated to reach optimal results on the overall cost and charge sustaining of battery. The effects of driving cycles, degradation states, and pricing scenarios were analyzed.*

Keywords: ECMS; fuel cell; hybrid system; EMS; degradation

I. INTRODUCTION

The design of an energy management strategy is critical to improving the fuel efficiency of a vehicle system with an alternative powertrain system, such as hybrid electric vehicles or fuel cell electric vehicles. In particular, in fuel cell electric vehicles, the energy management strategy should consider system degradation and fuel savings because the hardware cost of the fuel cell system is much higher than that of a conventional powertrain system. In this paper, an easily implantable near-optimal energy management controller is proposed. The proposed controller distributes power generation between the fuel cell and the battery to simultaneously minimize system degradation and fuel usage. The controller is designed to consider the degradation cost and fuel cost in the framework of the equivalent consumption minimization strategy concept. The proposed controller was validated with a fuel cell electric vehicle model in MATLAB/Simulink (MathWorks, Natick, MA, USA). The proposed control strategy showed significant overall cost reduction compared to a thermostat control strategy and a conventional Equivalent Consumption Minimization Strategy (ECMS) strategy

An energy management strategy (EMS) efficiently splits the power among different sources in a hybrid fuel cell vehicle (HFCV). Most of the existing EMSs are based on static maps while a proton exchange membrane fuel cell (PEMFC) has time-varying characteristics, which can cause mismanagement in the operation of a HFCV. This paper proposes a framework for the online parameters identification of a PEMFC model while the vehicle is under operation. This identification process can be conveniently integrated into an EMS loop, regardless of the EMS type. To do so, Kalman filter (KF) is utilized to extract the parameters of a PEMFC model online. Unlike the other similar papers, special attention is given to the initialization of KF in this work. In this regard, an optimization algorithm, shuffled frog-leaping algorithm (SFLA), is employed for the initialization of the KF. The SFLA is first used offline to find the right initial values for the PEMFC model parameters using the available polarization curve. Subsequently, it tunes the covariance matrices of the KF by utilizing the initial values obtained from the first step. Finally, the tuned KF is employed online to update the parameters. The ultimate results show good accuracy and convergence improvement in the PEMFC characteristics estimation

II. LITERATURE REVIEW

Studies on EMSs can be divided into the rule-based strategy (RBS) and optimization-based strategy (OBS) [3]. The heuristic rules are the core of the RBS. These rules can be expressed as the deterministic rules in deterministic rule-based strategies or fuzzy rules in fuzzy rule-based strategies. Based on these rules, the on/off of fuel cell, operating models of ESSs, and corresponding power of power sources are determined to make sure the normal operation of the vehicle. Load following strategy, operating mode control strategy and fuzzy logic control are typical RBSs. The RBSs can be easily designed by engineers based on their experience. The real-time implication of these RBSs is also simple and their resilience on different driving patterns is strong. But optimal results for the designed objectives of EMSs are hardly reached. In order to overcome the deficiency of the RBS, OBS is designed to optimize the operation of vehicles and achieve the optimal objectives. The general configuration of OBS includes one or more optimal objectives and certain constraints such as limiting the state of charge (SOC) of ESSs and power ranges of power sources. Based on the optimization horizons, OBS can be divided into the global OBS taking the whole driving cycle as optimization horizons and local OBS on the instantaneous sampling time. Dynamical programming (DP), genetic algorithm (GA) and particle swarm optimization are widely used algorithms to solve global optimization problems to achieve optimal objectives [4, 5]. Equivalent consumption minimization strategy, Pontryagin's minimum principle (PMP) and model predictive control (MPC) are typical local OBSs [6, 7]. Many studies on EMSs for FCHEVs only focus on the minimization of hydrogen consumption or equivalent hydrogen consumption from ESSs without sufficiently considering the degradation of fuel cell and battery. A small number of studies try to make a tradeoff between battery degradation and hydrogen consumption. For example, in [8] and [9] discrete dynamic programming and convex optimization are respectively used to optimize the costs of battery degradation and hydrogen consumption. But the fuel cell degradation is not considered into the optimal objectives of these studies. In [9], minimizing the hydrogen and fuel cell lifetime costs as the objective function is solved through stochastic dynamic programming (SDP). Three representative EMSs: DP, PMP, and MPC in [09] are developed to minimize hydrogen consumption and fuel cell durability. In [5] and [6], the fuel cell models are identified online to find the variation of fuel cell system performances and to operate the fuel cell in the best efficiency and power operating points through PMP. Battery degradation is not considered in the above researches. The deficiency for the above researches on the minimizing oval cost of FCHEVs can be concluded as not considering all power sources degradation. Fuzzy logic control optimized by GA in [5], MPC based sequential quadratic programming in [9] and DP in [6, 7] consider all hydrogen cost and degradation costs of fuel cell and battery. But empirical degradation models of fuel cell and battery used to calculate their degradation costs are not precise, which cannot describe the dynamical degradation rates of power sources under the dynamical conditions of vehicles like the changeable external environment condition, temperature, and operating conditions. The lifetime costs calculated based on the unprecise degradation rates bring a big challenge to the reliability of their developed EMSs. The deficiency for these researches can be defined as not reliable and precise lifetime cost estimation, which also occurs in the researches with the first deficiency. Furthermore, a common serious drawback in present researches is that the variable driving situations, state of health (SOH) of power sources and prices of hydrogen and power sources, which affect the optimal cost results and charge sustaining of battery, even more seriously, the normal operation of the vehicle, are totally not considered. The EMS control parameters optimized for specified driving cycles cannot meet all kinds of road situations. The degradation of power sources leads to the decrease of their performances and corresponding degradation rates will change along with SOHs [8]. Prices of hydrogen and power sources will also change along with their technology development on production, usage, investment, and operation. In a word, the constant parameters in the EMSs aiming to improve the economy of FCHEVs cannot meet the dynamical and variable operating conditions of FCHEVs, no matter in the external environment like variable driving conditions and prices or in the internal conditions like degradation and failures. Well known as an efficient and eco-friendly power source, fuel cell, unfortunately, offers slow dynamics. When attached as primary energy source in a vehicle, fuel cell would not be able to respond to abrupt load variations. Supplementing battery and/or supercapacitor to the system will provide a solution to this shortcoming. On the other hand, a current regulation that is vital for lengthening time span of the energy storage system is needed. This can be accomplished by keeping fuel cell's and batteries' current slope in reference to certain values, as well as attaining a stable dc output voltage. For that purpose, a feedback control system for regulating the hybrid of fuel cell, batteries, and super capacitor was constructed for this study. Output voltage of the studied hybrid power sources (HPS) was

administered by assembling three dc-dc converters comprising two bidirectional converters and one boost converter. Current/voltage output of fuel cell was regulated by boost converter, whereas the bidirectional converters regulated battery and super capacitor. Reference current for each converter was produced using Model Predictive Control (MPC) and subsequently tracked using hysteresis control. These functions were done on a controller board of a space DS1104. Subsequently, on a test bench made up from 6 V, 4.5 Ah battery and 7.5 V, 120 F super capacitor together with a fuel cell of 50 W, 10 A, experiment was conducted. Results show that constructing a control system to restrict fuel cell's and batteries' current slope and maintaining dc bus voltage in accordance with the reference values using MPC was feasible and effectively done.

III. PROPOSED ARCHITECTURE

To the best knowledge of the authors, no efforts have been made to develop a cost minimization strategy (CMS) to minimize the hydrogen cost and lifetime costs of power sources under variable internal and external conditions on power sources and road situations with adaptive control parameters. In order to bridge this research gap and overcome shortcomings of present researches on improving FCHEVs economy, an OCMS for FCHEVs based on decision making framework considering the dynamical road information, power sources degradation, price evolution of materials is developed. Three main original contributions can be concluded to distinguish our research from other exiting studies. First, a CMS is built to improve the fuel economy and decrease the lifetime costs of fuel cell and battery based on their degradation models. Second, a decision making framework, for the first time, is built composed of the driving pattern recognition-enabled decision making (DPRDM), prognostics-enabled decision making (PDM), and price prediction-enabled decision making (PPDM). Based on the DPRDM, real-time driving patterns can

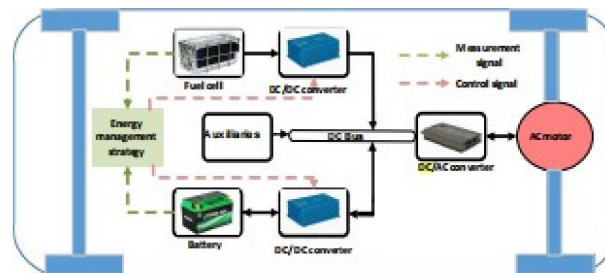


Fig. 1. Power train architecture.

be recognized through the support vector machine (SVM). Based on the PDM, the health states of fuel cell and battery are online estimated based on the unscented Kalman filter (UKF) and are further able to precisely calculate the lifetime costs of power sources cooperating with their empirical degradation models. Through the PPDM, the price evolutions of hydrogen and power sources until the end of the lifetime of the vehicle are projected based on the experience rate approach. Under the innovative decision making framework, the internal and external conditions of the vehicle can be determined. Third, the pre-optimal equivalent cost factors (ECFs) through the GA are calculated. Based on the recognized diving cycle, estimation of SOHs and price prediction, optimal ECFs and corresponding suitable control policies are adjusted to extend the lifetimes of fuel cell and battery, keep the charge sustaining of battery and achieve the minimization objective of the overall cost.

IV. FUEL CELL SYSTEM MODEL

Electrical model

The fuel cell stack, as the heart of the fuel cell system, converts chemical energy into electrical energy via the reaction of hydrogen and oxygen [20]. Due to the low voltage of a single cell, many cells combine to form a fuel cell stack (approximate 1V). The FCHEV employs a 370- cell PEMFC with a rated output of 114kW. The fuel cell stack voltage may be computed by multiplying the voltage of a single cell by the number of cells, as shown below:

$$E = N(E_{rev} - E_{act} - E_{ohm} - E_{con})$$

where N is the cell number, is the thermodynamic reversible potential, is the activation losses, is the ohmic losses, is the concentration losses. These potentials in the static state can be defined as follows:

$$E_{rev} = E_0 - 0.85e^{-3}(T - T_c) + \frac{RT}{2F} \ln(\sqrt{P_{O_2} P_{H_2}})$$

$$E_{act} = \frac{RT}{2\alpha F} \ln\left(\frac{I_{fc}}{I_0}\right)$$

$$E_{ohm} = I_{fc} R_{fc}$$

$$E_{con} = -B \ln\left(1 - \frac{I_{fc}}{I_m}\right)$$

where E_0 is the reversible nearest potential of a single cell and P_{O_2} and P_{H_2} are the partial pressures of oxygen and hydrogen respectively, T and T_c are the temperatures of fuel cell and temperature correction offset respectively, R is the ideal gas constant, F is Faraday constant, I_{fc} is fuel cell current, α is the symmetry factor, I_0 is the exchange current density, R_{fc} is the internal resistance, B is an empirical constant, I_m is the maximum allowed current.

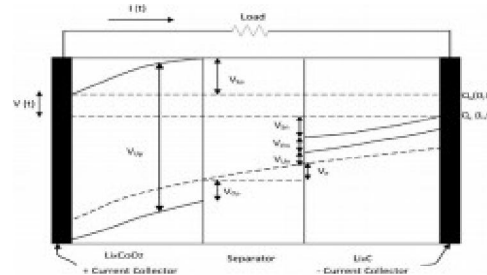


Fig.3. Battery Voltages

Figure 2 depicts the fuel cell output power and system efficiency, as well as currents. During the functioning of the fuel cell system, the hydrogen consumption rate may be defined as:

$$m_{H_2} = \int_0^t \frac{M_{H_2} N}{2F} I_{fc}(t) dt$$

where t is the running duration of the fuel cell system, M_{H_2} is the hydrogen molar mass, N is the cell number, and F is the Faraday constant

Degradation model

The depreciation of power sources is unavoidable as they operate. The deterioration of the fuel cell affects various elements, including catalyst layer degradation, membrane degradation, and gas diffusion layer degradation, resulting in a drop in fuel cell voltage and output power over the same amount of hydrogen input. One of the most significant goals of EMS is to minimise fuel cell deterioration in order to accomplish the economic goal. A degradation model is created to determine the deterioration rates of the fuel cell under different activities in order to estimate the degradation cost of the fuel cell.

The start/stop cycle, load shifting cycle, idling mode, and high power mode are the four operating states of a fuel cell. Their degradation rates are specified as constants. The deterioration rates of fuel cells tested under automotive circumstances, as well as the decay rates and currents of the fuel cells, exhibit a quadratic connection. Furthermore, the start/stop cycle causes a generally equivalent rise in fuel cell deterioration. As a result, a "always-on technique" is used to extend the life of the fuel cell.

The fuel cell empirical deterioration models, as well as its operating conditions, are constructed as follows:

$$V' = k \left((a \cdot I_{fc}^2 + b \cdot I_{fc} + c) \cdot t + V'_4 \cdot n_2 \right)$$

where a , b , and c are fitting coefficients, t is the sampling time, V'_4 is the deterioration rate when the load changes, and n_2 is the quick load-changing cycle time

Battery model

Electrochemistry model: The FCHEV's ESS is a lithium-ion battery pack with 198 cells and a nominal capacity of 1.6 kWh. Based on the current drawn from the battery, an electrochemistry-based battery model at the cell level is created to predict its voltage as a function of time. The battery is made up of positive and negative electrodes as well as

electrolyte. The potential difference between the positive and negative current collectors (minus resistance losses) determines the cell's total voltage. Figure 3 depicts the cell's potential as a result of several electrochemical operations. Has a full description of the modeling procedure. The following is the relationship between battery output voltage and different potentials:

$$V(t) = V_{U,p} - V_{O,p} - V_{U,n} - V_{O,n} - V_r$$

where and are the equilibrium potentials, and are the surface potentials, and is the ohmic potential owing to ohmic resistance at solid-phases (and), electrolytes (), and current collectors (and). Subscript and denote positive and negative values, respectively. The quantity of charge in the electrodes determines the equilibrium potential of each electrode as follows:

$$V_{U,i} = U_0 + \frac{RT}{nF} \ln\left(\frac{1-x_i}{x_i}\right) + V_{act,i}$$

$$V_{act,i} = \frac{1}{nF} \left(\sum_{k=0}^{N_i} A_{i,k} \left((2x_i - 1)^{k+1} - \frac{2x_i k (1-x_i)}{(2x_i - 1)^{1-k}} \right) \right)$$

where 0 denotes the reference voltage, T the electrode temperature, is the number of electrons transported in the reaction, is the activity coefficient term, is the empirical coefficient, and represents the subscript p or n. Surface and ohmic over potentials can be computed as follows:

$$V_{O,i} = \frac{RT}{F\alpha} \arcsin\left(\frac{J_i}{2j_{i0}}\right)$$

$$V_r = i_{app} R$$

where is the constant resistance, is the symmetry factor, is the current density, is the exchange current density, and is the current density. The charge percentage of the negative electrode and the entire battery is defined as the battery SOC:

$$SOC = \frac{q_n}{0.6 q_{max}}$$

where is the total quantity of Li ions, and is the amount of Li ions in the negative electrode.

Degradation model:

The deterioration of a battery is difficult and impacted by a variety of elements such as time, temperature, discharge rate, and depth of discharge. To measure battery degradation, including calendar ageing and cycle ageing, an empirical degradation model is utilised. The total capacity loss Q_{loss} , which includes both the capacity loss Q_{loss} calendar and the capacity loss Q_{loss} cycle owing to cycle ageing, is defined as:

$$Q_{loss} = Q_{loss}^{cycle} + Q_{loss}^{calendar}$$

$$Q_{loss}^{calendar} = At^{0.5} e^{-\frac{E}{RT}}$$

$$Q_{loss}^{cycle} = (aT^2 + bT + c) e^{(dT+e)lr_{rate}} Ah_{to}$$

where is the activation energy, is the gas constant, is the absolute temperature, is time, is the charging/discharging rate represented as C rate, and h represents the Ah throughput.

V. VALIDATION AND RESULT ANALYSIS

Many circumstances can be made up of varying driving cycles, health statuses, and pricing. The combined UDDS and UNIF01 driving cycles are used to validate the OCMS (CUU). As examples of different ageing states and pricing, three degradation conditions of fuel cells and batteries (D1, D2, and D3) and three price circumstances on the years 2020, 2025, and 2030 (P1, P2, and P3) were chosen. Situation 1 (S1) is assigned to D1 and P1, situation 2 (S2) to D2 and P2, and situation 3 (S3) to D3 and P3 in the CUU driving cycle, as indicated in Table III. Table IV shows the best ECFs for three circumstances under six different driving cycles (from 1 to 6). The ECFs may be automatically changed through

the decision making framework based on the optimal ECFs in various conditions to seek the best overall cost and charging sustaining outcomes. The driving pattern of the CUU driving cycle may be detected using the DPRDM, as shown in Fig. 14. For the recognition process, two-time factors for the DPRDM combined with moving windows should be mentioned. The duration of the output recognised pattern and the time length of the movement horizon for previous data to identify the present driving pattern are set to 60s and 10s, respectively. Once the driving cycle pattern has been determined, the relevant ECF from the pre-optimized library is chosen till the next prediction time. Table V compares the simulation results for CMS with constant ECF (labelled CMS) with OCMS with adaptive ECF (labelled OCMS) in three scenarios. It should be noted that, in order to create a fair comparison, the final battery SOC fluctuation should also be incorporated in the total cost through the extra battery sustaining charge cost in addition to the overall cost at the conclusion of the driving cycle (17). In comparison to CMS (ECF=0.621), OCMS' total expenses have grown by 0.9 percent, 1.9 percent, and 15 percent for S1, S2, and S3, respectively. OCMS respects the charge maintaining of the battery by observing same SOC at the conclusion of the driving cycle, although this goal is not met by OCMS. The decrease in total expenses from S1 to S3 is attributable to lower hydrogen, fuel cell, and battery prices, as well as time. Figure 15 depicts the hydrogen consumption cost, fuel cell lifetime cost, battery lifetime cost, total cost, and battery SOC for OCMS, as well as the driving cycle under S1. In comparison to hydrogen and fuel cells, the cost of battery deterioration is the highest. The SOC of the battery is likewise restricted. Figure 16 depicts the power splits as well as the driving cycle for OCMS under S1. The fuel cell generally runs at low power. The battery is significantly responsible for the dynamical change of load power. Both the fuel cell and the battery operate in a restricted power range.

Using the Newton's second law of motion, the vehicle acceleration can be expressed as

$$\frac{dV}{dt} = \frac{\sum F_t - \sum F_{resistance}}{\delta M}$$

where V = vehicle speed

$\sum F_t$ = total tractive effort [Nm] $\sum F_{resistance}$ = total resistance [Nm]

M = total mass of the vehicle [kg]

δ = mass factor for converting the rotational inertias of rotating components into translational mass

Engine speed ratio defined as

$$v = \frac{n_n}{n(T_{max})}$$

where n_n = engine speed at maximum power, also known as nominal speed

$n(T_{max})$ = engine speed at maximum torque

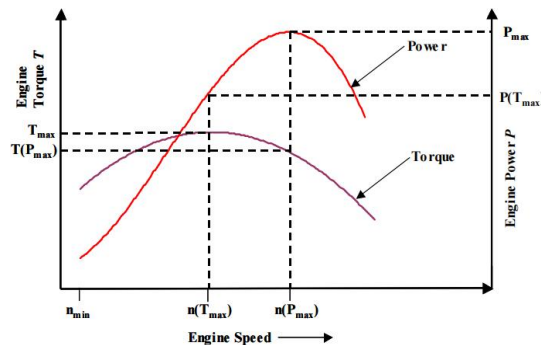


Figure : Characteristic curves of an internal combustion engine

Drive train tractive effort and vehicle speed

After having dealt with the configuration of the drive train, this section deals with the tractive effort. The torque transmitted from the power plant to the driven wheels (T_w) is given by:

$$T_u = i_g i_e \eta_t T_p \quad (1)$$

where

i_3 = gear ratio of the transmission (1)

i_0 = gear ratio of the final drive

η_t = efficiency of the driveline from the power plant to the driven wheels

T_2 = torque output from the power plant [Nm]

The tractive effort on the driven wheels (Figure 9) is expressed as

$$F = \frac{T_m}{r_{dx}^n} \quad (2)$$

where r_{dyp} = dynamic radius of the tire [m]

Substituting value of T_w from equation 1 into equation 2 gives

$$F_t = \frac{T_p i_g i_0 \eta_t i_l}{r_{dypn}} \quad (3)$$

The total mechanical efficiency of the transmission between the engine output shaft and driven wheels is the product of the efficiencies of all the components of the drive train. The rotating speed of the driven wheel is given by

$$N_s = \frac{N_p}{i_g i_a^i} [rpm] \quad (4)$$

where N_p = rotational speed of the transmission [rpm]

The rotational speed N_p of the transmission is equal to the engine speed in the vehicle with a manual transmission and the turbine speed of a torque converter in the vehicle with an automatic transmission. The translation speed of the wheel (vehicle speed) is expressed as

$$V = \frac{\pi N_p r_{dm}}{30} [m/s] \quad (5)$$

By substituting the value of N_w from equation 4 into equation 5, the vehicle speed can be expressed as

$$V = \frac{\pi N_p r_{dm}}{30 i_g i_a^i} [m/s] \quad (6)$$

Acceleration Performance

The acceleration of a vehicle is defined by its acceleration time and distance covered from zero speed to a certain high speed on a level ground. The acceleration of the vehicle can be expressed as

$$\begin{aligned} a &= \frac{dV}{dt} = \frac{F_t - F_f - F_s}{M\delta} \\ &= \frac{T_p i_0 i_g n_l / r_{dm} - Mg_r - 1/2 \rho_a C_D A_f V^2}{M\delta} \\ &= \frac{a}{\delta} (d - f_r) \end{aligned}$$

where δ is the rotational inertia factor taking into account the equivalent mass increase due to the angular moments of the rotating components. This mass factor can be written as

$$\delta = 1 + \frac{I_v}{Mr_{um}^2} + \frac{i^2 i^2 I_p}{Mr^2}$$

I_S = total angular inertial moment of the wheels

I_p = total angular inertial moment of the rotating components associated with the power plant

To determine the value of δ , it is necessary to determine the values of the mass moments of inertia of all the rotating parts. In case the mass moments of inertia are not available then, the rotational factor (δ) can be approximated as:

$$\delta = 1 + \delta_1 + \delta_2 i^2$$

$$\delta_1 \approx 0.04$$

$$\delta_2 \approx 0.0025$$

The acceleration rate along with vehicle speed for a petrol engine powered vehicle with a four gear transmission and an electric motor powered vehicle with a single gear transmission are shown as follows:

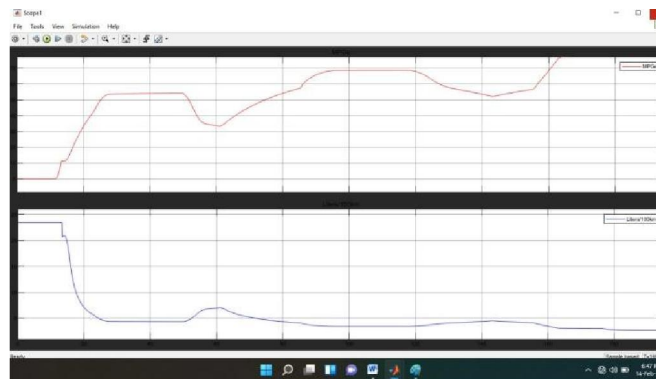


Fig.. EV Fuel Output

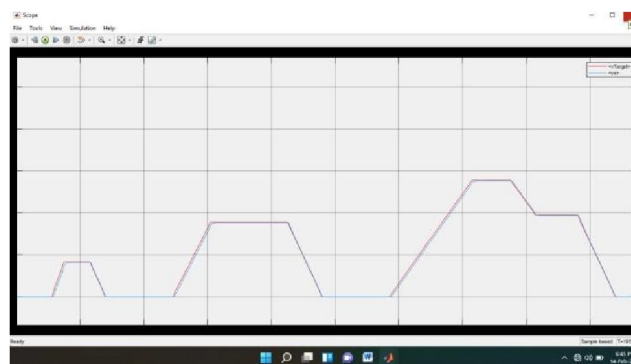


Fig.. EV Drive Profile

VI. CONCLUSION

This paper developed a cost optimal, decision making energy management strategy considering the fuel cell and battery lifetimes and the uncertainty on the driving pattern, degradation states of power sources, and prices of fuel and drivetrain components. The overall cost including the hydrogen cost, fuel cell and battery degradation cost was minimized. The decision making framework was built to supply optimal equivalent cost factors at all kinds of situations on the driving pattern, health state and price. Simulation results proved that the optimal cost and charger sustaining of battery were achieved through the cooperation between CMS and decision making framework composing the OCMS.

REFERENCES

- [1] Amin, R. T. Bambang, A. S. Rohman, C. J. Dronkers, R. Ortega, and A. Sasongko, "Energy Management of Fuel Cell/Battery/Supercapacitor Hybrid Power Sources Using Model Predictive Control," *IEEE Transactions on Industrial Informatics*, vol. 10, no. 4, pp. 1992-2002, 2014
- [2] Y. Xing, J. Na, and R. Costa-Castelló, "Real-Time Adaptive Parameter Estimation for a Polymer Electrolyte Membrane Fuel Cell," *IEEE Transactions on Industrial Informatics*, vol. 15, no. 11, pp. 6048-6057, 2019.
- [3] H. Li, A. Ravey, A. N'Diaye, and A. Djerdir, "A novel equivalent consumption minimization strategy for hybrid electric vehicle powered by fuel cell, battery and supercapacitor," *Journal of Power Sources*, vol. 395, pp. 262- 270, 2018.
- [4] T. Liu, H. Yu, H. Guo, Y. Qin, and Y. Zou, "Online Energy Management for Multimode Plug-In Hybrid Electric Vehicles," *IEEE Transactions on Industrial Informatics*, vol. 15, no. 7, pp. 4352-4361, 2019.
- [5] K. Jia, Y. Chen, T. Bi, Y. Lin, D. Thomas, and M. Sumner, "Historical-Data-Based Energy Management in a Microgrid With a Hybrid Energy Storage System," *IEEE Transactions on Industrial Informatics*, vol. 13, no. 5, pp. 2597-2605, 2017.
- [6] J. P. Torreglosa, P. García, L. M. Fernández, and F. Jurado, "Predictive Control for the Energy Management of a Fuel-Cell–Battery– Supercapacitor Tramway," *IEEE Transactions on Industrial Informatics*, vol. 10, no. 1, pp. 276- 285, 2014.
- [7] H. Li, A. Ravey, A. N'Diaye, and A. Djerdir, "Online adaptive equivalent consumption minimization strategy for fuel cell hybrid electric vehicle considering power sources degradation," *Energy Conversion and Management*, vol. 192, pp. 133-149, 2019.
- [8] F. Martel, S. Kelouwani, Y. Dubé, and K. Agbossou, "Optimal economy-based battery degradation management dynamics for fuel-cell plug-in hybrid electric vehicles," *Journal of Power Sources*, vol. 274, pp. 367-381, 2015.
- [9] X. Hu, L. Johannesson, N. Murgovski, and B. Egardt, "Longevity-conscious dimensioning and power management of the hybrid energy storage system in a fuel cell hybrid electric bus," *Applied Energy*, vol. 137, pp. 913-924, 2015.